2014

The Dearth of Neutral Hydrogen in Galactic Dwarf Spheroidal Galaxies

Kristine Spekkens

Natasha Urbancic

Brian S. Mason

Beth Willman
Haverford College, bwillman@haverford.edu

The Astrophysical Journal Letters, 795:L5 (5pp), 2014 November 1 doi:10.1088/2041-8205/795/1/L5

THE DEARTH OF NEUTRAL HYDROGEN IN GALACTIC DWARF SPHEROIDAL GALAXIES

Kristine Spekkens[1], Natasha Urbancic[1], Brian S. Mason[2], Beth Willman[3], and James E. Aguirre[4]
[1] Department of Physics, Royal Military College of Canada, P.O. Box 17000, Station Forces, Kingston, Ontario K7K 7B4, Canada; kristine.spekkens@rmc.ca
[2] National Radio Astronomy Observatory, 520 Edgemont Road, Charlottesville, VA 22903-2475, USA
[3] Haverford College, 370 Lancaster Avenue, Haverford, PA 19041, USA
[4] Department of Physics and Astronomy, University of Pennsylvania, 209 South 33rd Street, Philadelphia, PA 19104, USA
Received 2014 September 23; accepted 2014 September 27; published 2014 October 13

ABSTRACT

We present new upper limits on the neutral hydrogen (H I) content within the stellar half-light ellipses of 15 Galactic dwarf spheroidal galaxies (dSphs), derived from pointed observations with the Green Bank Telescope (GBT) as well as Arecibo *L*-band Fast ALFA survey and Galactic All-Sky Survey data. All of the limits $M_{\rm H\,I}^{\rm lim}$ are more stringent than previously reported values, and those from the GBT improve upon constraints in the literature by a median factor of 23. Normalizing by *V*-band luminosity L_V and dynamical mass $M_{\rm dyn}$, we find $M_{\rm H\,I}^{\rm lim}/L_V \sim 10^{-3}\,M_\odot/L_\odot$ and $M_{\rm H\,I}^{\rm lim}/M_{\rm dyn} \sim 5\times10^{-5}$, irrespective of location in the Galactic halo. Comparing these relative H I contents to those of the Local Group and nearby neighbor dwarfs compiled by McConnachie, we find that the Galactic dSphs are extremely gas-poor. Our H I upper limits therefore provide the clearest picture yet of the environmental dependence of the H I content in Local Volume dwarfs. If ram pressure stripping explains the dearth of H I in these systems, then orbits in a relatively massive Milky Way are favored for the outer halo dSph Leo I, while Leo II and Canes Venatici I have had a pericentric passage in the past. For Draco and Ursa Minor, the interstellar medium mass that should accumulate through stellar mass loss in between pericentric passages exceeds $M_{\rm H\,I}^{\rm lim}$ by a factor of ∼30. In Ursa Minor, this implies that either this material is not in the atomic phase, or that another mechanism clears the recycled gas on shorter timescales.

Key words: galaxies: dwarf – galaxies: evolution – radio lines: galaxies

Online-only material: color figures

1. INTRODUCTION

The origin and evolution of the Milky Way's dwarf galaxy satellites address several problems in cosmological galaxy formation (e.g., Weinberg et al. 2013). In particular, their gas content provides an important clue to their evolutionary histories: it has long been appreciated that dwarf spheroidal galaxies (dSphs), preferentially located within the virial radius of the Milky Way, tend to be deficient in neutral hydrogen (H I) compared to the dwarf irregulars located farther out (e.g., Einasto et al. 1974; Lin & Faber 1983). A variety of searches for H I in the Galactic dSphs have been performed over the years (e.g., Knapp et al. 1978; Blitz & Robishaw 2000; Bouchard et al. 2006; Grcevich & Putman 2009, hereafter GP09). Although some detections have been claimed (e.g., Carignan et al. 1998; Blitz & Robishaw 2000; Bouchard et al. 2006), most were not confirmed by deeper observations (see the discussion in GP09). These non-detections suggest that environmental processes play a key role in shaping the morphologies of Galactic dSphs. Stringent upper limits on the H I content of the latter may elucidate the details of these mechanisms, as well as the basic Milky Way and dSph properties on which they depend.

The H I content of nearby dwarf galaxies has been examined most recently by GP09, who used non-detections in reprocessed H I Parkes All-Sky Survey (HIPASS; Putman et al. 2003) data and in Leiden–Argentine–Bonn (LAB; Kalberla et al. 2005) survey data to constrain Galactic accretion rates due to satellite infall. However, the sensitivities of those surveys[5] produce relatively weak upper limits on the faintest nearby dSphs, while those for dSphs in the outer halo do not strongly exclude characteristic values of gas-rich Local Volume dwarfs farther out. Pointed observations with large single dishes such as the Robert C. Byrd Green Bank Telescope (GBT) have the potential to search for H I down to much lower levels, and higher sensitivity and spectral resolution surveys such as the Arecibo Legacy Fast ALFA Survey (ALFALFA; Giovanelli et al. 2005) and the Galactic All-Sky Survey (GASS; McClure-Griffiths et al. 2009), respectively, are also now available. These developments warrant a re-examination of the H I content of the Galactic dSphs, which we carry out here for the subset of that population that are well separated in velocity from the Milky Way's H I disk and high-velocity clouds (HVCs).

2. SAMPLE SELECTION AND OBSERVATIONS

We examine the H I content of all dSphs within 300 kpc of the Galactic center that have the following.

1. Distances *D* and radial velocities $V_{\rm LSR}$ measured from resolved stellar population studies.
2. A value of $V_{\rm LSR}$ that does not fall in the velocity range of either Galactic disk or HVC H I emission along the dSph line of sight in the deepest available data.

Comparing to the Milky Way subgroup compilation of McConnachie (2012, hereafter M12), the first criterion omits Pisces II from our sample for its lack of a measured $V_{\rm LSR}$. The second criterion provides a "clean" sample in which to search for H I down to low levels. It excludes Canis Major, Segue II, Hercules, Willman I, and Ursa Major I because $V_{\rm LSR}$ overlaps with the Galactic H I disk, as well as Fornax, Sculptor, and Leo IV because $V_{\rm LSR}$ falls in the velocity range of known HVC complexes (GP09; Moss et al. 2013). We find faint high-velocity gas

[5] Errors in the H I mass equations in GP09 imply that the upper limits they derive from HIPASS and LAB data are underestimated by factors of ∼20 and ∼15, respectively.

Table 1
New H I Limits for dSphs

Name	$D_\odot$[a] (kpc)	$V_{\rm LSR}$[a] (km s^{-1})	L_V[a] ($L_\odot$)	r_h[a] (arcmin)	ϵ[a]	σ_*[a] (km s^{-1})	H I Source	σ_{15} (mJy beam^{-1})	$M_{\rm H\,I}^{\rm lim}$ ($M_\odot$)	$M_{\rm H\,I}^{\rm lim}/L_V$ ($M_\odot/L_\odot$)	$M_{\rm H\,I}^{\rm lim}/M_{\rm dyn}$
(1)	(2)	(3)	(4)	(5)	(6)	(7)	(8)	(9)	(10)	(11)	(12)
Milky Way											
Segue I	23	203	3.4E2	4.4	0.48	3.9	GBT	1.1	11	3.1E-2	4.1E-5
Sagittarius dSph	26	149	2.2E7	340	0.64	11.4	BL99	23	4430	2.1E-4	2.3E-5
Ursa Major II	32	−113	4.1E4	16	0.63	6.7	GBT	2.0	74	1.8E-3	1.9E-5
Bootes II	42	−107	1.0E3	4.2	0.21	10.5	GBT	1.2	38	3.7E-2	1.2E-5
Coma Berenices	44	104	3.7E3	6.0	0.38	4.6	GBT	1.8	62	1.7E-2	6.5E-5
Bootes III	47	210	1.8E4	48[b]	0.50[b]	14.0	ALFALFA	2.0	1080	6.1E-2	1.5E-5
Bootes I	66	110	2.8E4	13	0.39	2.4	GBT	1.6	252	8.9E-3	3.1E-4
Draco	76	−274	2.8E5	10	0.31	9.1	GBT	0.75	133	4.7E-4	1.2E-5
Ursa Minor	76	−233	2.8E5	8.2	0.56	9.5	GBT	0.61	63	2.2E-4	6.6E-6
Sextans	86	216	4.5E5	28	0.35	7.9	GASS	29	9430	2.1E-2	3.8E-4
Carina	105	204	3.7E5	8.2	0.33	6.6	GASS	24	4780	1.3E-2	7.6E-4
Leo V	178	171	1.0E4	2.6	0.50	3.7	GBT	0.72	403	3.9E-2	3.7E-4
Canes Venatici I	218	42	2.4E5	8.9	0.39	7.6	GBT	0.98	1170	4.9E-3	6.1E-5
Leo II	233	78	7.1E5	2.6	0.13	6.6	ALFALFA	2.0	1960	2.8E-3	4.3E-4
Leo I	254	277	5.4E6	3.4	0.21	9.2	ALFALFA	2.2	3560	6.6E-4	3.0E-4
Local Group											
Cetus	755	−88	2.8E6	3.2	0.33	8.3	GASS	23	2.3E5	8.3E-2	4.4E-3
Tucana	887	188	5.6E5	1.1	0.48	15.8	GASS	21	2.9E5	5.2E-1	3.5E-3
Andromeda XVIII	1213	−325	5.0E5	0.92	...[c]	9.7	LAB	183	4.8E6	9.5E0	2.7E-1

Notes. Column 1: dSph name; Column 2: distance from the Sun; Column 3: Systemic velocity $V_{\rm LSR}$ of the stellar component in the LSRK frame; Column 4: V-band luminosity corrected for Galactic extinction; Column 5: elliptical half-light radius r_h; Column 6: ellipticity ϵ of the stellar component; Column 7: velocity dispersion of the stellar component; Column 8: source of the single-dish H I spectrum: ALFALFA, GASS, LAB, BL99 or our own GBT data; Column 9: rms noise of the H I spectrum at 15 km s^{-1} resolution, at $V_{\rm LSR}$; Column 10: $5\sigma_{15}$ upper limit on the H I mass; Column 11: upper limit on the ratio of H I mass to L_V; Column 12: upper limit on the ratio of H I mass to dynamical mass $M_{\rm dyn}$.
[a] Taken from M12 unless otherwise noted.
[b] Approximate values from Grillmair (2009).
[c] No estimate available. Because $r_h \ll \theta$ for the LAB survey, $N_b = 1$ in Equation (2) irrespective of the value of ϵ.

at $-200\,{\rm km\,s^{-1}} < V_{\rm LSR} < -100\,{\rm km\,s^{-1}}$ in our GBT spectra of Canes Venatici I (CVn I) and Canes Venatici II; $V_{\rm LSR}$ of the latter dSph falls in this velocity range, and we therefore omit it from the sample. We discuss the potential impact of our selection criteria on our conclusions in Section 5.

The basic properties of the 15 Galactic dSphs that satisfy our selection criteria are given in Table 1. Unless otherwise noted, we use the measured stellar properties compiled by M12 (2013 May 30 database version) for all systems.

We examine the H I environment of each sample dSph using GASS or ALFALFA survey data where available, or using LAB data otherwise. Assuming that any putative H I in these systems is in dynamical equilibrium, we expect the width of this distribution to resemble that of the stars. To maximize our sensitivity to this H I signal, we therefore smooth all spectra to a resolution of 15 km s^{-1}, which corresponds to the characteristic stellar velocity distribution width in the sample dSphs (see Table 1). We examine the most sensitive survey data available at $V_{\rm LSR}$ near the stellar centroid of each dSph, and find no H I emission. The 21.0′ resolution H I maps near the Sagittarius dSph by Burton & Lockman (1999, hereafter BL99) are deeper than the GASS data at that location, and we therefore use their non-detection to compute upper limits for this dSph. Since the GASS and LAB surveys also afford new H I limits on the Local Group dSphs Cetus, Tucana, and Andromeda XVIII, we include them at the bottom of Table 1.

We obtained deep, pointed GBT H I observations for a subset of the sample in 2014 May and 2014 June (program AGBT14A_284). We used the GBT Spectrometer with a bandpass of 12.5 MHz and 1.56 kHz channels centered at $V_{\rm LSRK} = 0$ to obtain an "on" spectrum along the line of sight to each dSph, as well as an off-target reference spectrum of equal integration time to subtract from the "on" scan and flatten the spectral baseline. For dSphs with half-light diameters $2r_h$ that exceed the 9.′1 FWHM θ of the GBT beam, additional offset pointings of comparable depth were obtained to fully sample the optical half-light ellipse $\pi(1-\epsilon)r_h^2$, where ϵ is the ellipticity of the stellar distribution. The data were reduced using the standard GBTIDL[6] routine *getps* and smoothed to a resolution of 15 km s^{-1}.

We find no H I emission at $V_{\rm LSR}$ of the dSphs targeted by our GBT observations. The source of the most sensitive 15 km s^{-1} resolution H I spectrum at the location of each sample dSph, and the rms noise σ_{15} per beam of that spectrum at $V_{\rm LSR}$ are given in Columns 8 and 9 of Table 1, respectively.

3. CALCULATING H I LIMITS

We use the non-detection at $V_{\rm LSR}$ of each dSph to compute upper limits on the H I mass within its half-light ellipse. The H I mass $M_{\rm H\,I}$ of a detected source is given by

$$M_{\rm H\,I} = 2.36 \times 10^{-4} D^2 \int S dV \; M_\odot, \quad (1)$$

where D is the distance to the source in kiloparsecs and $\int S\,dV$ is the integrated H I flux across the source in mJy km s^{-1}. We compute 5σ, 15 km s^{-1} width upper limits on the H I mass within the half-light ellipse of each dSph:

$$M_{\rm H\,I}^{\rm lim} = 0.0177\, D^2\, \sigma_{15} \sqrt{N_b}\; M_\odot, \quad (2)$$

[6] http://gbtidl.nrao.edu/

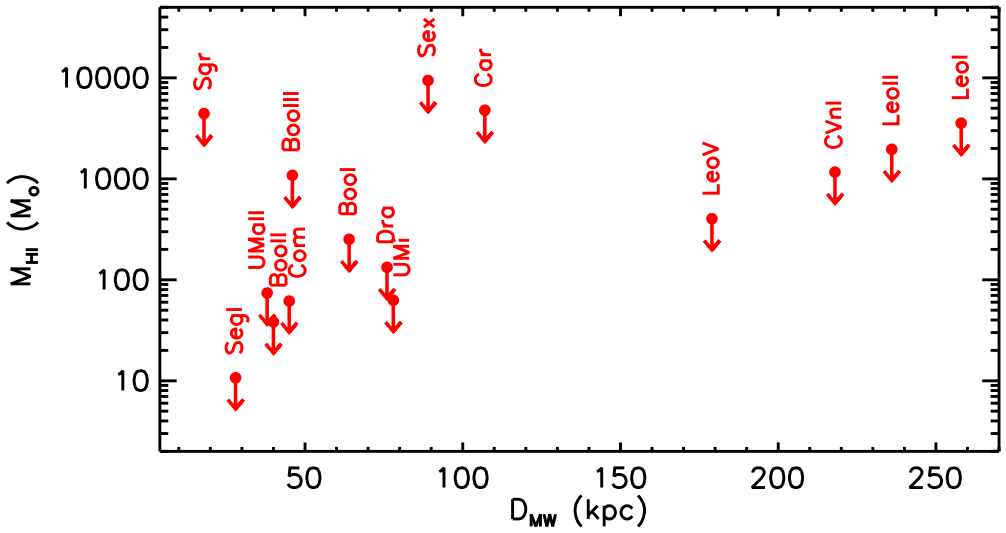

Figure 1. Upper limits on the H I masses of Galactic dSphs within their half-light ellipses, plotted as a function of Galactocentric distance.
(A color version of this figure is available in the online journal.)

where σ_{15} is the rms noise in mJy beam^{-1} of the 15 km s^{-1} resolution spectrum at $V_{\rm LSR}$. In Equation (2), N_b is the number of beams across the source, rounded up to the nearest integer:

$$N_b = \left\lceil \frac{2.77(1-\epsilon)r_h^2}{\theta^2} \right\rceil, \quad (3)$$

where $\theta = 9.'1$ for our GBT spectra, $\theta = 4.'0$ for ALFALFA (Giovanelli et al. 2005), $\theta = 16'$ for GASS (Kalberla et al. 2010), and $\theta = 40'$ for LAB (Kalberla et al. 2005). The values of $M_{\rm HI}^{\rm lim}$ for the sample dSphs are given in Column 10 of Table 1, and are plotted in Figure 1 as a function of Galactocentric distance $D_{\rm MW}$.

4. RESULTS: NEW H I LIMITS FOR GALACTIC dSphs

The H I limits that we calculate for Galactic dSphs are in the range $11\,M_\odot < M_{\rm HI}^{\rm lim} < 9430\,M_\odot$ (Table 1); all of them are more stringent than previously reported values. In particular, $M_{\rm HI}^{\rm lim}$ derived from our GBT observations yield tighter upper limits than corresponding values in the literature by factors ranging from 1.01 (Bailin & Ford 2007, for Bootes I) to 610 (GP09, for CVn I, after correcting for errors in their limiting H I mass relations), with a median improvement of a factor of 23.

Figure 2 shows $M_{\rm HI}^{\rm lim}$ normalized by (1) V-band luminosity L_V, and (2) dynamical mass $M_{\rm dyn}$ within the half-light radius as a function of $D_{\rm MW}$. We use the relation of Walker et al. (2009) to compute $M_{\rm dyn}$ from the stellar kinematics of each dSph, as compiled by M12:

$$M_{\rm dyn} = 580\, r_h\, \sigma_*^2 \;\; M_\odot, \quad (4)$$

where σ_* is the stellar velocity dispersion in km s^{-1} and r_h is in parsecs.

Since $M_*/L_V \sim 1\,M_\odot/L_\odot$ for the old, metal-poor stellar populations characteristic of many dSphs (e.g., Martin et al. 2008), Figure 2(a) effectively plots $M_{\rm HI}^{\rm lim}/M_*$. Uncertainties in the initial mass function and stellar evolution of the faintest dwarfs should move the points by less than ∼0.5 dex (Martin et al. 2008; Geha et al. 2013).

To compare the H I content of the sample dSphs to that of more isolated nearby systems, we also plot $M_{\rm HI}/L_V$ and $M_{\rm HI}/M_{\rm dyn}$ for Local Volume dwarfs in Figure 2. We consider all dwarfs classified as Local Group satellites or nearby neighbors in M12 as our reference, omitting only Phoenix because the H I detected near it is offset from the stellar distribution by $\gtrsim 0.5\,r_h$ (Young et al. 2007). The dotted vertical line in Figure 2 shows the approximate virial radius of the Milky Way, $R_{\rm vir} = 300$ kpc (e.g., Klypin et al. 2002).

To compute $M_{\rm HI}/L_V$ for the Local Volume dwarfs, we take the H I detection and luminosity information directly from M12. Only 4/37 systems are not detected in H I: we plot $M_{\rm HI}^{\rm lim}/L_V$ for them using our new limits for Cetus, Andromeda XVIII, and Tucana (Table 1), and the 5σ upper limit $M_{\rm HI}^{\rm lim} = 8\times10^4\,M_\odot$ for KKR 25 obtained by Begum & Chengalur (2005).

We also plot $M_{\rm HI}/M_{\rm dyn}$ or $M_{\rm HI}^{\rm lim}/M_{\rm dyn}$ for the 27/37 Local Volume dwarfs where stellar or H I kinematics have been measured. We use stellar kinematics where available, and use the H I kinematics otherwise; for systems with detected rotation V_r, we substitute $\sigma_*^2 \rightarrow \sigma^2 + V_r^2$ in Equation (4). More sophisticated estimates of $M_{\rm dyn}$ could be obtained by examining the kinematics of each system in detail, but are unlikely to differ from those in Figure 2(b) by more than ∼0.5 dex.

Figure 2 shows that we find $M_{\rm HI}^{\rm lim}/L_V \sim 10^{-3}\,M_\odot/L_\odot$ and $M_{\rm HI}^{\rm lim}/M_{\rm dyn} \sim 5\times10^{-5}$ for the dSphs, for all $D_{\rm MW} < R_{\rm vir}$. Our upper limits therefore conclusively demonstrate that if there is any H I in these systems, it is negligible compared to both their stellar and dynamical masses. By contrast, most Local Volume dwarfs have relative H I contents $M_{\rm HI}/L_V \sim 1\,M_\odot/L_\odot$ and $M_{\rm HI}/M_{\rm dyn} \sim 0.1$. Our values of $M_{\rm HI}^{\rm lim}$ for the sample dSphs therefore imply that they are extremely gas-poor relative to the bulk of the Local Volume dwarfs.

5. DISCUSSION

The environmental dependence of the H I content of Local Group galaxies is well known (see Section 1), but Figure 2 presents the clearest picture yet of this phenomenon. Our data show, for the first time, that, notwithstanding the Magellanic System (Brüns et al. 2005), Cetus, Tucana, and KKR 25, the transition between gas-rich and gas-poor dwarfs in the vicinity of the Milky Way is abrupt and located near $R_{\rm vir}$. Even our weakest upper limits imply that $M_{\rm HI}/L_V$ and $M_{\rm HI}/M_{\rm dyn}$ for the sample dSphs are at least ∼100 and ∼1000 times lower than

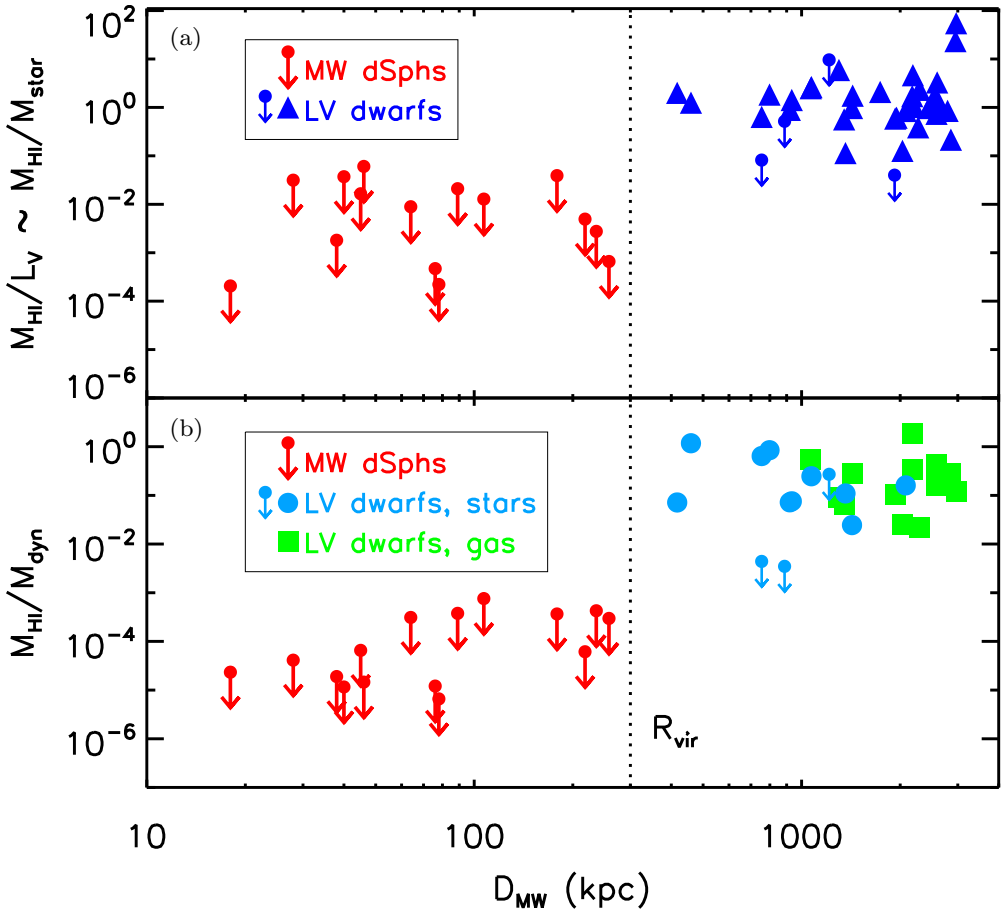

Figure 2. H I content of the Milky Way dSphs and Local Volume dwarfs, normalized by (a) V-band luminosity L_V ($\sim$ the stellar mass M_*), and (b) dynamical mass $M_{\rm dyn}$. In panel (a), the red arrows show $M_{\rm H\,I}^{\rm lim}/L_V$ for the sample Milky Way dSphs, and the blue filled triangles and arrows show $M_{\rm H\,I}/L_V$ and $M_{\rm H\,I}^{\rm lim}/L_V$, respectively, for systems classified as Local Group satellites or nearby neighbors by M12. In panel (b), the red arrows show $M_{\rm H\,I}^{\rm lim}/M_{\rm dyn}$ for the sample Milky Way dSphs, where $M_{\rm dyn}$ is computed from stellar kinematics. The light blue filled circles and arrows show $M_{\rm H\,I}/M_{\rm dyn}$ and $M_{\rm H\,I}^{\rm lim}/M_{\rm dyn}$ for Local Volume satellites, respectively, where $M_{\rm dyn}$ is computed from stellar kinematics. The green filled squares show $M_{\rm H\,I}/M_{\rm dyn}$ for Local Volume satellites where gas kinematics are used to compute $M_{\rm dyn}$. The vertical dotted line in both panels shows the approximate virial radius of the Milky Way, $R_{\rm vir} = 300$ kpc.

(A color version of this figure is available in the online journal.)

the characteristic value for Local Volume dwarfs, irrespective of their distance from the Galactic center.

For this study, we selected only the 15/26 Galactic dSphs with $V_{\rm LSR}$ that do not overlap with the Milky Way's H I disk or HVC emission (see Section 2). This produces a "clean" sample from an H I search perspective, but also raises the possibility that the excluded dSphs contain gas in excess of the $M_{\rm H\,I}^{\rm lim}/L_V$ and $M_{\rm H\,I}^{\rm lim}/M_{\rm dyn}$ reported here. Our cursory examination of the GASS and LAB data for these objects indicates that this is not the case. GP09 reached a similar conclusion using HIPASS data, classifying H I clouds claimed to be associated with Sculptor (Carignan et al. 1998) and Fornax (Bouchard et al. 2006) as ambiguous detections. None of these clouds lie within the half-light ellipse of the dSph in its vicinity.

dSphs at a given $D_{\rm MW}$ exhibit a range of $V_{\rm LSR}$ because they are bound to the Milky Way (e.g., M12), and the latter's H I disk and HVCs fill a sizeable fraction of the spatial and spectral search volume (e.g., Peek et al. 2011; Moss et al. 2013): an overlap in $V_{\rm LSR}$ between Galactic H I clouds and dSph stars is therefore unlikely to imply a physical association between them. An investigation of the H I content of dSphs in these confused fields requires deep, wide-field H I mapping, and even then associating H I features with stellar systems at the same location is not straightforward (e.g., Carignan et al. 1998; Bouchard et al. 2006; Grcevich & Putman 2009). We defer a detailed examination of the H I content of the dSphs confused with Galactic emission to a future publication (K. Spekkens et al. in preparation), but argue that the dearth of H I in the sample presented here is likely representative of the Galactic dSph population as a whole.

Ram pressure stripping is thought to explain the absence of H I in the Galactic dSphs relative to Local Volume dwarfs (e.g., Lin & Faber 1983; Blitz & Robishaw 2000; GP09), though tidal effects (e.g., Read et al. 2006; Mayer et al. 2006), resonances (e.g., D'Onghia et al. 2009), and feedback from star formation (e.g., Gatto et al. 2013) may also play a role. Gatto et al. (2013) show that numerical simulations are needed to accurately model gas stripping. Nonetheless, a scaling of the analytic Gunn & Gott (1972) criterion reasonably describes the conditions under which ram pressure stripping occurs in dSph progenitors:

$$\rho_{\rm MW} v_{\rm orb}^2 \gtrsim 5 \rho_d \sigma_*^2 \,, \qquad (5)$$

where $\rho_{\rm MW}$ and ρ_d are the densities of the hot halo gas and dSph interstellar medium (ISM), and $v_{\rm orb}$ is the dSph orbital velocity. The small $M_{\rm H\,I}^{\rm lim}$ for the outer halo dSphs CVn I, Leo II, and Leo I reported here imply that this condition must be met at some point in their orbits (see also GP09).

Adopting $\rho_d \sim 0.1$ cm^{-3} characteristic of Leo T (Ryan-Weber et al. 2008), recent estimates of the coronal density

profiles of the Milky Way (Anderson & Bregman 2010; Gatto et al. 2013; Marinacci et al. 2014) combined with Equation (5) favor the pericenter distances and velocities of Leo I implied by a Milky Way mass $M_{\rm vir} \gtrsim 1.5 \times 10^{12}\ M_\odot$, at the higher end of the accepted range (Sohn et al. 2013). Similarly, the narrow range in subhalo orbital velocities in cosmological simulations of Milky-Way-sized halos (Boylan-Kolchin et al. 2013) suggests that, even if CVn I and Leo II are on their first infall, ram pressure stripping is not effective at their present $D_{\rm MW}$. Like Leo I, CVn I and Leo II have therefore likely had a pericentric passage in the past that has taken them to $D_{\rm MW} \lesssim 100$ kpc. More detailed calculations are needed to refine these arguments (e.g., Gatto et al. 2013), but they illustrate the implications of the $M_{\rm H\,I}^{\rm lim}$ presented here for outer halo dSph orbits as well as for the basic properties of the Milky Way.

As expected from Equation (2), we obtain the tightest H I constraints for nearby, unresolved ($N_b = 1$) systems, which probe how gas is recycled into the ISM of the dSphs themselves. Assuming that a low-mass star in an old (>10 Gyr) stellar population losses ~0.3 $M_\odot$ of material after turning off the main sequence, Moore & Bildsten (2011) estimate a mass-loss rate of $\dot{M} \sim 5 \times 10^{-12}\ M_\odot\ {\rm yr}^{-1}\ {L_\odot}^{-1}$. A $L \sim 10^4\ L_\odot$ dSph with an orbital period $T \sim 1$ Gyr therefore accumulates ~50 $M_\odot$ of interstellar material from stellar evolution before ram pressure sweeps away the gas at pericenter; this mass is of the same order as $M_{\rm H\,I}^{\rm lim}$ for several sample dSphs.

Our non-detections in UMi and Draco are particularly interesting in this respect, since their L_V (Table 1) combined with their respective $T \sim 1$ Gyr and $T \sim 5$ Gyr inferred from proper motions (Lux et al. 2010) imply an accumulation of interstellar material that exceeds $M_{\rm H\,I}^{\rm lim}$ by a factor of ~30. Draco is close to pericenter and thus may have just lost this gas to ram pressure, but UMi is not (Lux et al. 2010). As is the case in globular clusters (e.g., van Loon et al. 2006), $M_{\rm H\,I}^{\rm lim}$ in UMi therefore requires either that the ISM accumulated between pericentric passages is not in the atomic phase, or that another mechanism clears the recycled gas on shorter timescales.

6. CONCLUSIONS

Using a combination of pointed observations from the GBT as well as ALFALFA and GASS survey data, we have presented new upper limits on the H I content within the half-light ellipses of the 15 Galactic dSphs for which $V_{\rm LSR}$ does not overlap with Galactic H I disk or HVC emission. Our non-detections imply values of $M_{\rm H\,I}^{\rm lim}$ that are more stringent than those available in the literature for all sample dSphs, while our GBT spectra improve upon previous limits by median factor of 23. We find upper limits on the relative H I content of the dSphs to be $M_{\rm H\,I}^{\rm lim}/L_V \sim 10^{-3}\ M_\odot/L_\odot$ and $M_{\rm H\,I}^{\rm lim}/M_{\rm dyn} \sim 5 \times 10^{-5}$ for all $D_{\rm MW} < R_{\rm vir}$: any H I present in these systems is clearly negligible compared to both their stellar and dynamical masses. We compare the relative H I content of the dSph sample to that of the Local Group and nearby neighbor dwarfs compiled by M12. With few exceptions, these Local Volume dwarfs are gas-rich with $M_{\rm H\,I}/L_V \sim 1\ M_\odot/L_\odot$ and $M_{\rm H\,I}/M_{\rm dyn} \sim 0.1$, and the sample dSphs are extremely gas-poor by comparison.

Our data show, for the first time, that the transition between gas-rich and gas-poor dwarfs near the Galaxy is abrupt and located near $R_{\rm vir}$, in the clearest picture yet of the environmental dependence of their H I content. Assuming that ram pressure stripping is the dominant mechanism responsible for this phenomenon, we discuss how the dearth of H I in outer halo dSph Leo I favors orbits for that dwarf in a relatively massive Milky Way, while that for Leo II and CVn I implies that these dSphs have had a pericentric passage in the past. We also discuss how the ISM accumulated in dSphs between pericentric passages due to stellar mass loss exceeds $M_{\rm H\,I}^{\rm lim}$ for the nearby dSphs Draco and UMi by a factor of ~30. In UMi, this implies that either this material is not in the atomic phase or that another mechanism clears the recycled gas on shorter timescales.

We thank R. Giovanelli and M. P. Haynes for their help accessing the ALFALFA survey data, and P. Kalberla for his help with the GASS server. K.S. acknowledges support from the Natural Sciences and Engineering Research Council of Canada. This work was supported by NSF grant AST-1151462 to B.W. The National Radio Astronomy Observatory is a facility of the National Science Foundation operated under cooperative agreement by Associated Universities, Inc.

Facility: GBT

REFERENCES

Anderson, M. E., & Bregman, J. N. 2010, ApJ, 714, 320
Bailin, J., & Ford, A. 2007, MNRAS, 375, L41
Begum, A., & Chengalur, J. N. 2005, MNRAS, 362, 609
Blitz, L., & Robishaw, T. 2000, ApJ, 541, 675
Bouchard, A., Carignan, C., & Staveley-Smith, L. 2006, AJ, 131, 2913
Boylan-Kolchin, M., Bullock, J. S., Sohn, S. T., Besla, G., & van der Marel, R. P. 2013, ApJ, 768, 140
Brüns, C., Kerp, J., Staveley-Smith, L., et al. 2005, A&A, 432, 45
Burton, W. B., & Lockman, F. J. 1999, A&A, 349, 7
Carignan, C., Beaulieu, S., Côté, S., Demers, S., & Mateo, M. 1998, AJ, 116, 1690
D'Onghia, E., Besla, G., Cox, T. J., & Hernquist, L. 2009, Natur, 460, 605
Einasto, J., Saar, E., Kaasik, A., & Chernin, A. D. 1974, Natur, 252, 111
Gatto, A., Fraternali, F., Read, J. I., et al. 2013, MNRAS, 433, 2749
Geha, M., Brown, T. M., Tumlinson, J., et al. 2013, ApJ, 771, 29
Giovanelli, R., Haynes, M. P., Kent, B. R., et al. 2005, AJ, 130, 2598
Grcevich, J., & Putman, M. E. 2009, ApJ, 696, 385
Grillmair, C. J. 2009, ApJ, 693, 1118
Gunn, J. E., & Gott, J. R., III. 1972, ApJ, 176, 1
Kalberla, P. M. W., Burton, W. B., Hartmann, D., et al. 2005, A&A, 440, 775
Kalberla, P. M. W., McClure-Griffiths, N. M., Pisano, D. J., et al. 2010, A&A, 521, A17
Klypin, A., Zhao, H., & Somerville, R. S. 2002, ApJ, 573, 597
Knapp, G. R., Kerr, F. J., & Bowers, P. F. 1978, AJ, 83, 360
Lin, D. N. C., & Faber, S. M. 1983, ApJL, 266, L21
Lux, H., Read, J. I., & Lake, G. 2010, MNRAS, 406, 2312
Marinacci, F., Pakmor, R., Springel, V., & Simpson, C. M. 2014, MNRAS, 442, 3745
Martin, N. F., de Jong, J. T. A., & Rix, H.-W. 2008, ApJ, 684, 1075
Mayer, L., Mastropietro, C., Wadsley, J., Stadel, J., & Moore, B. 2006, MNRAS, 369, 1021
McClure-Griffiths, N. M., Pisano, D. J., Calabretta, M. R., et al. 2009, ApJS, 181, 398
McConnachie, A. W. 2012, AJ, 144, 4
Moore, K., & Bildsten, L. 2011, ApJ, 728, 81
Moss, V. A., McClure-Griffiths, N. M., Murphy, T., et al. 2013, ApJS, 209, 12
Peek, J. E. G., Heiles, C., Douglas, K. A., et al. 2011, ApJS, 194, 20
Putman, M. E., Staveley-Smith, L., Freeman, K. C., Gibson, B. K., & Barnes, D. G. 2003, ApJ, 586, 170
Read, J. I., Wilkinson, M. I., Evans, N. W., Gilmore, G., & Kleyna, J. T. 2006, MNRAS, 367, 387
Ryan-Weber, E. V., Begum, A., Oosterloo, T., et al. 2008, MNRAS, 384, 535
Sohn, S. T., Besla, G., van der Marel, R. P., et al. 2013, ApJ, 768, 139
van Loon, J. T., Stanimirović, S., Evans, A., & Muller, E. 2006, MNRAS, 365, 1277
Walker, M. G., Mateo, M., Olszewski, E. W., et al. 2009, ApJ, 704, 1274
Weinberg, D. H., Bullock, J. S., Governato, F., Kuzio de Naray, R., & Peter, A. H. G. 2013, arXiv:1306.0913
Young, L. M., Skillman, E. D., Weisz, D. R., & Dolphin, A. E. 2007, ApJ, 659, 331